Dynamic range models improve the near-term forecast for a marine species on the move

Alexa L. Fredston[1,2]*, Daniel Ovando[3]*, Lucas da Cunha Godoy[4], Jude Kong[5], Brandon Muffley[6], James T. Thorson[7], Malin L. Pinsky[4,2]

March 2025

*Co-first authors

[1] Department of Ocean Sciences, University of California, Santa Cruz, fredston@ucsc.edu

[2] Department of Ecology, Evolution, and Natural Resources, Rutgers University

[3] Inter-American Tropical Tuna Commission, dovando@iattc.org

[4] Department of Ecology and Evolutionary Biology, University of California Santa Cruz, mpinsky@ucsc.edu

[5] Dalla Lana School of Public Health, University of Toronto, jude.kong@utoronto.ca

[6] Mid-Atlantic Fishery Management Council, bmuffley@mafmc.org

[7] National Oceanic and Atmospheric Administration, james.thorson@noaa.gov

Statement of authorship: MLP and BM conceived of the project. ALF and DO gathered data. ALF, DO, MLP, JK, and JTT designed the model. ALF, DO, and LdCG implemented and evaluated the model. ALF wrote the first draft of the manuscript. All authors contributed to revisions.

Data accessibility statement: All data and code for this project are publicly available at: https://github.com/afredston/mid_atlantic_forecasts. The data and code repository from GitHub will be deposited into the Open Science Framework (OSF) with a stable DOI when the manuscript is accepted.

Running title: Mechanistic models predict fish range shifts

Keywords: ecological forecasting, mechanistic modeling, species distribution, species redistribution

Article type: Letter

Word counts: Abstract: 148, Main text: 5356, Text boxes: NA

Number of references: 67

Number of figures, tables, and text boxes: Figures: 6, Tables: 0, Text boxes: 0

Corresponding author: Alexa Fredston, 1156 High St, Earth & Marine Sciences Bldg A455, Santa Cruz, CA 95064. Phone: 831-459-2563. Fax: 831-459-4882. E-mail: fredston@ucsc.edu.

Abstract

Population dynamic models are widely used to predict demography. However, they have rarely been extended to biogeographical applications despite widespread calls to do so. We developed a process-based dynamic range model (DRM) that estimated demographic rates and the effects of the environment on demographic rates to forecast species range shifts in response to temperature change. As a proof of concept, we fitted DRMs to historical observations of summer flounder (*Paralichthys dentatus*), a fish species in the Northwest Atlantic, and evaluated model skill at retrospective forecasting. The best DRMs outperformed a statistical species distribution model and a persistence forecast at predicting biogeographical dynamics across a decade. The DRM approach is general and can be applied to a wide range of species with historical observations across space and time. By explicitly modeling demographic processes and their relationship to climate, DRMs promise to substantially advance prediction of species on the move.

Introduction

Prediction has become a central goal of ecology (Mouquet et al., 2015). Predictive ecology often seeks to forecast human impacts on ecosystems. It supports biodiversity conservation, natural resource management, climate change mitigation and adaptation, and other ecological applications (Urban et al., 2016). Near-term forecasting is a particularly pressing need so that the timescale of ecological information aligns with the often-short timescale of environmental decision-making (Dietze et al., 2018).

Species distributions have been a major emphasis of predictive ecology, particularly in the context of climate change (Pearson & Dawson, 2003). Species are shifting their ranges in response to climate change (Parmesan & Yohe, 2003), with cascading effects on communities, ecosystems, ecosystem services, and human welfare and well-being (Pecl et al., 2017). Early species distribution models (SDMs) projected species ranges and range shifts using correlations between species' presence (and sometimes abundance) and environmental variables (Elith & Leathwick, 2009). However, observed range shifts have been highly individ-

ualistic and are not well predicted by simple environmental variables (Davis et al., 1998; Rubenstein et al., 2023). SDMs have been critiqued in the context of near-term forecasting because they assume species are in equilibrium with the environment, may be trained on data that does not resemble future climates, and have demonstrated limited forecast skill to date (Jarnevich et al., 2015; Lee-Yaw et al., 2022). New approaches (e.g., hybrid and ensemble SDMs) are addressing some of these shortcomings, but still using fundamentally correlative approaches that do not explicitly model ecological mechanisms (Brodie et al., 2022; Ehrlén & Morris, 2015; Kearney & Porter, 2009; Zurell, 2017).

Mechanistic or "process-based" models are often presented as a way forward in forecasting range shifts and for predictive ecology in general (Dietze et al., 2018; Urban et al., 2016). These models can estimate assumed causal relationships, predict effects using those estimates, provide insight into fundamental ecological mechanisms, estimate parameters of interest, falsify ecological theories, and incorporate processes over varying spatial and temporal scales (Cabral et al., 2017; Evans et al., 2016). Another advantage of mechanistic models is that, if implemented in a hierarchical framework, they can model the underlying ecological processes separately from the data collection process, facilitating more accurate parameter estimation and error partitioning (Laubmeier et al., 2020). Mechanistic models are rare in biogeography, however, partly due to the heightened difficulty of parameter estimation and scale when mechanistic ecological models (e.g., population dynamic models) are made spatial (Briscoe et al., 2019).

One promising class of mechanistic models for range forecasting is dynamic range models (DRMs), which are spatially explicit population dynamic models that estimate demographic rates as a function of the environment (Pagel & Schurr, 2012). DRMs estimate key parameters from data on species' occurrences and abundances and can incorporate processes at multiple spatial and temporal scales, making them flexible tools that may be applied to a broad suite of ecological questions. However, this flexibility also makes them reliant on the availability of large datasets through time and space. Indeed, DRMs have mainly been fitted to simulated data for this reason (Zurell et al., 2016). DRMs have yielded useful results when applied to real data for parameter inference (Le Squin et al., 2021; Osada et al., 2019). However, DRMs have not been operationalized for range forecasting of real species—the main purpose for which they were designed (Briscoe et al., 2019; Pagel & Schurr, 2012).

An ideal system in which to operationalize DRMs for range forecasting is one where species have already shifted their ranges, where large-scale biodiversity surveys have been operating for some time, and where a strong theoretical understanding exists of the underlying population dynamics and how they relate to the environment. One such system is temperate marine continental shelf ecosystems. Range shifts have been particularly rapid and widespread in these systems, because there are relatively few barriers to dispersal, species live close to their thermal limits, and spatial gradients in temperature are less steep in the oceans than they are on land (Pinsky et al., 2020). Marine systems are also relatively data-rich: due to the historical and current significance of ma-

rine fisheries, we have records of historical fishing mortality, insights into the population dynamics of harvested marine species, and large-scale, long-term monitoring programs that have conducted scientific marine surveys in the U.S. for many decades (Maureaud et al., 2023).

Here, we built DRMs—mechanistic models that explicitly model demographic processes from physiological (i.e., temperature impacts on recruitment and survival) to metapopulation (i.e., dispersal) scales—to forecast range dynamics in response to climate variability and change using more than four decades of biogeographical data. We implemented these DRMs as hierarchical Bayesian models fitted to historical data from 1972-2006 on summer flounder (*Paralichthys dentatus*), an important commercial and recreational species on the east coast of the U.S. that has been shifting northward (Perretti & Thorson, 2019). We then evaluated DRM performance with a retrospective forecast from 2007-2016. We modeled the data collection process separately from the underlying ecological dynamics and quantified both process and measurement error. We designed a suite of candidate DRMs representing different hypotheses about the underlying ecological processes; this allowed us to explore which vital rates were most strongly affected by changing temperatures and the value of incorporating additional ecological complexity (Briscoe et al., 2019; Zurell et al., 2016). Specifically, we compared DRMs with temperature-dependent recruitment, mortality, or movement. We also compared DRM forecasts to predictions from a SDM and a persistence forecast. Out-of-sample DRM forecasts were more accurate and less biased than the SDM or the persistence forecast at predicting range centroid and edge positions over a decade of testing.

1 Methods

The DRM simulated age-structured population dynamics, including dispersal, within a spatial domain that was discretized into habitat patches along the coastline, such that each patch was adjacent to one or two neighboring patches (Fig. 1). We also discretized time, with data from 1972 - 2016. Model parameters were estimated by fitting this process-based model to observations of species abundance density across space and time. We implemented a base model without temperature-dependent demographic rates and three models with temperature-dependent recruitment, mortality, or movement. In our presentation of the models, we denote vectors, matrices, and arrays in bold.

We used a hierarchical Bayesian approach to model observed numerical densities ($\mathbf{D}$, representing the density of all individuals regardless of age) as a function of the modeled latent age-structured population density ($N_{p,a,t}$) for each patch (p), age class (a), and time step (t). Observed presence ($\mathbf{P}$) was also incorporated to help account for zero-density patches.

Our methodology comprises two parts: a process model, which explicitly models the underlying population dynamics, and an observation model, which relates these dynamics to observed data. We first describe the options for the process model, followed by the observation model, which remained consistent

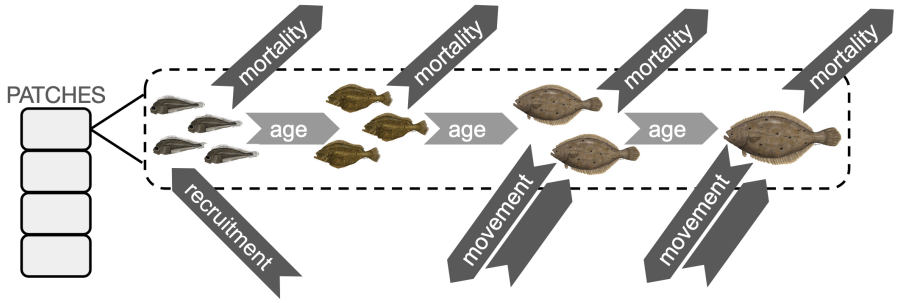

Figure 1: Schematic of the patch structure and temperature-dependent processes in the DRM design highlighting dynamics within an example patch. All patches contained distinct age classes and experienced stochastic recruitment. The three processes for which a temperature effect could be implemented are shown as dark grey arrows. Temperature-dependent recruitment affected the production of recruits by adults; temperature-dependent mortality affected all age classes; and temperature-dependent movement affected the dispersal of adults between adjacent patches.

across all process model configurations.

1.1 Process models

1.1.1 Base model

The base process model included age structure, adult dispersal, stochastic recruitment, and annual mortality. In particular, the population dynamics driving $N_{p,a,t}$ were as follows. First, the recruitment (i.e., production of age 1 individuals) in each year and patch was calculated as a stochastic process (Johnson et al., 2016) around a long-term average:

$$N_{p,a=1,t} = \mu \times e^{r_t - \frac{\sigma^2_{\text{proc}}}{2}} \tag{1}$$

where μ is the average density of recruitment per patch across all space and time, r_t represents recruitment stochasticity (through a first-order autoregressive process), and σ_{proc} is its conditional standard deviation. Equation (1) implies that recruitment in a given year is the same for all patches. The autoregressive term r_t was defined as

$$r_t = \alpha r_{t-1} + \sigma_{\text{proc}} z_t, \tag{2}$$

where z_t is an uncorrelated standard Normal error term and α is the temporal autocorrelation, namely the correlation between r_t and r_{t-1}.

We then modeled adults and juveniles (the latter are older than recruits but not yet mobile or reproductive) separately. Summer flounder reache maturity around two years of age (NEFSC, 2019), so in our application, age class one

represented recruits, age class two represented juveniles, and age classes three and older represented adults. Juvenile age classes were modeled as the fraction of the next youngest age class that survived to the following year in a given patch:

$$N_{p,a,t} = N_{p,a-1,t-1} \times s_{a-1,t-1} \tag{3}$$

where s represents annual survival proportion, which was constant across patches unless we added temperature-linked survival (as explained later). Because summer flounder experience fishing mortality, we combined age- and year-specific fishing mortality $f_{a,t}$ with natural mortality m to calculate survival fraction:

$$s_{a,t} = e^{-(f_{a,t}+m)}. \tag{4}$$

Both m and $f_{a,t}$ are instantaneous rates, so they can exceed 1.

Adults differed from juveniles in that they could move among adjacent patches. We calculated age-structured population density for adults with an isotropic dispersal fraction δ among adjacent patches:

$$\begin{aligned} N_{p,a,t} = (1-2\delta)N_{p,a-1,t-1} \times s_{a-1,t-1} \\ +\delta N_{p-1,a-1,t-1} \times s_{a-1,t-1} \\ +\delta N_{p+1,a-1,t-1} \times s_{a-1,t-1}. \end{aligned} \tag{5}$$

Edges were treated as reflective, so adults did not disperse beyond the model domain and dispersal rates were adjusted accordingly at the edges. Therefore, we specified $N_{p,a,t} = (1-\delta)N_{p,a-1,t-1} \times s_{a-1,t-1} + \delta N_{p-1,a-1,t-1} \times s_{a-1,t-1}$ in the northern-most patch, and $N_{p,a,t} = (1-\delta)N_{p,a-1,t-1} \times s_{a-1,t-1} + \delta N_{p+1,a-1,t-1} \times s_{a-1,t-1}$ in the southern-most patch.

1.1.2 Temperature effects

To incorporate the effects of temperature on population dynamics—and, consequently, on species distributions over space and time—we designed a series of alternative models for temperature dependence. These represented different hypotheses describing how temperature may affect population dynamics. For example, adults might move to track their preferred thermal conditions, and indeed, marine species ranges are highly correlated with their physiological thermal tolerances (Sunday et al., 2012). However, the distribution of recruits has shifted north faster than adults for some species, suggesting that temperature might instead affect recruitment into the age 1 cohort (Perretti & Thorson, 2019). Other research indicates that historical population dynamics are consistent with temperature effects on natural mortality (O'Leary et al., 2019). To explore these three hypotheses in the context of range shifts, we implemented alternative models that included temperature effects on (1) recruitment, (2) mortality, or (3) adult movement. To avoid parameter identifiability issues, these temperature effects were tested in separate models and were not combined, noting that in reality temperature could affect multiple processes at the same time.

In each case, we calculated a relative index of temperature suitability for each patch and year, $\mathbf{I}$. $\mathbf{I}$ was maximized at an optimal temperature, τ, which was estimated as part of model fitting. The intuition behind τ depends on the model structure. In the recruitment model, τ was the temperature at which recruitment was highest. In the mortality model, it represented the temperature at which natural mortality was lowest. The movement model represented the temperature toward which the greatest proportion of fish migrated from an adjacent patch. $\mathbf{I}$ was calculated as a Gaussian function such that, as the actual temperature $\mathbf{T}$ deviated from τ, the temperature suitability index $\mathbf{I}$ declined at a rate inversely proportional to a width parameter ω,

$$I_{p,t} = e^{\left(-0.5(\frac{T_{p,t}-\tau}{\omega})^2\right)}. \tag{6}$$

The temperature-dependent recruitment model linked temperature to recruitment by using $\mathbf{I}$ to rescale $N_{p,a=1,t}$, thus modifying Equation (1):

$$N_{p,a=1,t} = \mu \times e^{r_t - \frac{\sigma^2_{\text{proc}}}{2}} \times I_{p,t}. \tag{7}$$

In this case, μ becomes the average density of recruits under optimal environmental conditions, that is, when $T = \tau$.

To model temperature-dependent mortality, we modified Equation (4) to include the temperature effect $\mathbf{I}$, which acted by reducing survival when the temperature was not at τ:

$$s_{p,a,t} = e^{-(f_{a,t}+m+\gamma(1-I_{p,t}))}, \tag{8}$$

where γ is the excess natural mortality due to temperature. Note that, unlike in Equation (4), s could now vary over p because the temperature effect led to distinct survival across patches.

The movement model required more complexity because we modeled both the passive diffusion between patches in Equation (5), δ, and taxis—i.e., the directed movement by adults in response to environmental gradients. We followed the methods in Thorson *et al.* (2021). Specifically, we calculated a log-transformed version of $\mathbf{I}$ and constructed a p-by-p taxis matrix $\mathbf{X}$ for each year by subtracting the $\mathbf{I}$ of adjacent patches and multiplying the difference (i.e., the habitat gradient) by β_{tax}, a parameter that defined how much taxis changed per unit of temperature. A p-by-p diffusion matrix, $\mathbf{Z}$, simply included δ for adjacent patches (rescaled so that columns in the matrix summed to 1 at the end) and zeros elsewhere. We then summed and exponentiated $\mathbf{Z}$ and $\mathbf{X}$ in every year to yield the movement matrix $\mathbf{M} = e^{\mathbf{X}+\mathbf{Z}}$ containing annual movement fractions between each patch. This matrix was used to redistribute adults among patches rather than Equation (5), with the mortality rates in Equation (4) applied. In other words, we calculated $N_{p,a,t}$ in this model configuration by multiplying the right-hand side of Equation (5) by $\mathbf{M}$.

1.2 Observation model

The observation model related the observed densities to the process model. In particular, we defined observed presence ($\mathbf{P}$) from observed density ($\mathbf{D}$) at patch p and time t as

$$P_{p,t} = \begin{cases} 1 & \text{if } D_{p,t} > 0 \\ 0 & \text{if } D_{p,t} = 0. \end{cases} \tag{9}$$

We assumed $P_{p,t}$ and $D_{p,t}$, respectively, were distributed as follows

$$P_{p,t} \sim \text{Bernoulli}(\theta_{p,t}) \tag{10}$$

$$(\log(D_{p,t}) \mid P_{p,t} = 1) \sim \mathcal{N}\left(\log(\lambda_{p,t}/\theta_{p,t}) - \frac{\sigma^2_{\text{obs}}}{2}, \sigma_{obs}\right), \tag{11}$$

where $\theta_{p,t}$ is the probability of encountering individuals at site p and time t, $\mathcal{N}$ indicates a normal distribution, σ_{obs} is the standard deviation of $\log(D_{p,t})$, and $\lambda_{p,t} = \sum_a N_{p,a,t}$ is the latent density of individuals in each patch. Note that we divided $\lambda_{p,t}$ by $\theta_{p,t}$ in Equation (11) to ensure that the expectation of their product was equal to the mean of the observed abundance densities ($\mathbf{D}$).

A logit-link was used to connect the probabilities of encounter $\theta_{p,t}$ to the predicted densities as follows

$$\text{logit}(\theta_{p,t}) = \beta_0 + \beta_1 \log(\lambda_{p,t}), \tag{12}$$

where β_0 and β_1 are slope and intercept parameters controlling how much the probability of the species being encountered increases with the true population density.

1.3 Model implementation

We wrote the DRM in Stan, a platform for Bayesian modeling (Team, 2022), and used "cmdstanr" (Gabry et al., 2024) to produce the results in R (Supp. Tab. 1). We specified weakly informative priors for parameters α, β_0, β_1, σ_{obs}, and δ. We also bounded them to ecologically meaningful values: β_1 was restricted to positive numbers, and δ was restricted to the interval $[0, 1/3]$ because the probability of an individual staying in place or moving to one of two adjacent patches cannot exceed 100%. For temperature dependent models, we also specified weakly informative priors for the respective additional parameters included in the model (Supp. Tab. 2). We specified fishing and natural mortality rates as known values from a stock assessment in most model configurations (see Section 1.4 for details).

For each model configuration, we obtained samples from the posterior from four parallel chains, each of which ran for 5,000 iterations, including 2,000 warm-up iterations. We considered a model to have converged if less than 5% of the transitions in the sampler after warm-up were reported as divergent.

1.4 Data

To evaluate the DRMs, we used data from National Oceanic and Atmospheric Administration (NOAA) bottom trawl surveys conducted in the northeast U.S. since 1968 (Smith, 2002). These surveys have been conducted with standardized equipment and methods over time, and utilize a stratified randomized sampling design, making them ideal for climate biogeography applications (Fredston et al., 2021; Fredston-Hermann et al., 2020; Pinsky et al., 2013). We downloaded the 2020 release of OceanAdapt, a data portal that compiled North American bottom trawl survey records (Forrest et al., 2020). The NOAA Northeast survey operates in fall and spring; we used the fall survey that more often catches summer flounder.

The sampling unit for the survey is a single "haul", an event during which a fishing net is towed through the ocean for a fixed amount of time. Temperature is measured *in situ* for each haul at the seafloor. After each haul, scientists on board the survey vessel identify, count, weigh, and measure the catch in the net. To ensure that the years analyzed were sampled consistently throughout time, we used data from 1972-2016.

These records encompassed the region from Cape Hatteras in North Carolina to the border between Canada and Maine (Fig. 2), from just north of 35°N to above 44°N. To model spatial structure in the region, we divided the summer flounder data into 10 patches, each 1°latitude in height (Fig. 2). We calculated the observed summer flounder density $\mathbf{D}$ in units of fish per haul. We calculated $D_{p,t}$ as the average number of summer flounder per haul in patch p in year t. These observed density values—varying over space and time—were the main data input to the DRM.

The ability of the survey gear to catch summer flounder individuals depends on their size. To relate this observation effect to the age structure in the DRM, we converted density-at-age to density-at-length using a length-at-age key. This key assumes that summer flounder, on average, grow according to a von Bertalanffy curve with log-normal deviations and a constant coefficient of variation of 20%. Using this key, we converted density of fish at a given age a to density of fish at length. From there, we assumed that the survey gear had a logistic selectivity curve, with the lengths at 50% and 95% selectivity estimated by the model. This selectivity curve was then used to convert the age-structured density of fish in the model ($N_{p,a,t}$) to the expected density of fish caught by the survey ($\lambda_{p,t}$):

$$\lambda_{p,t} = \sum_a \Phi(a) N_{p,a,t} \tag{13}$$

with the function $\Phi(a)$ encoding the probability of sampling an individual of age a.

We aggregated temperature data to the patch level by taking a mean of all bottom temperature values from hauls in that patch and year. *In situ* sea bottom temperature data was missing for some hauls, including all hauls south of 38°N in 2008. To fill this data gap, we fitted a linear mixed-effects model

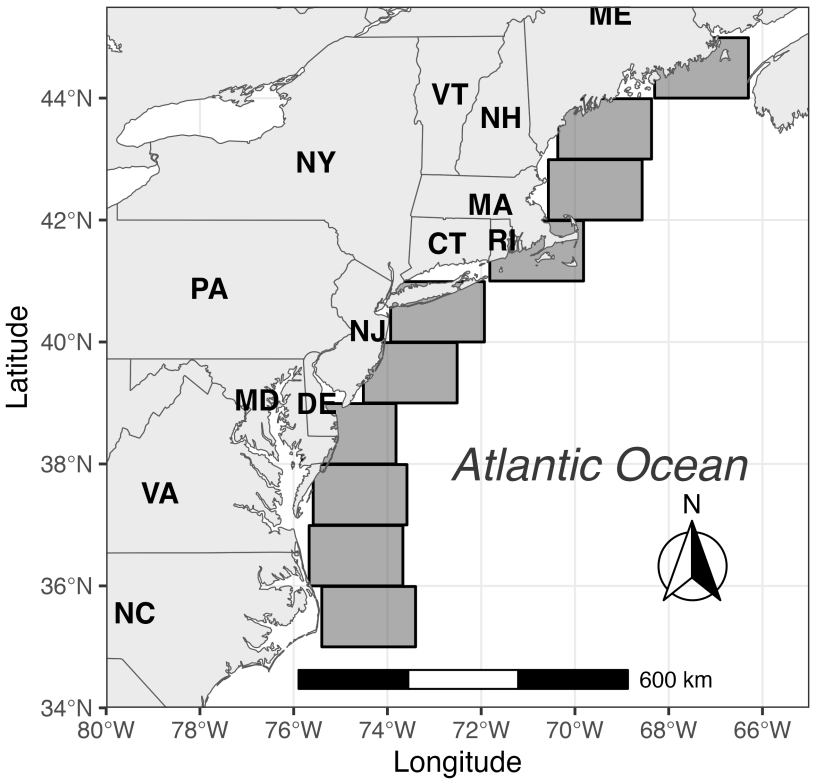

Figure 2: Map of the study region showing the modeled patches as grey boxes. Each patch was 1°latitude high. U.S. states are labeled for reference.

with latitude as a fixed effect, year as a random effect, and all available bottom temperature data as the response variable. We then used this fitted model to predict bottom temperature in 2008 in the three patches with missing data.

Summer flounder in the northeast U.S. have a stock assessment—a statistical analysis that integrates multiple data sources to produce estimates of total biomass, fishery catch rates, and other parameters to inform fisheries management. We used the estimated natural mortality rate m (often assumed to be constant for all years and age-classes) and fishing mortality-at-age $f_{a,t}$ (which differed across years t and age-classes a) from a recent stock assessment for this summer flounder population (NEFSC, 2019). The stock assessment fixed $m = 0.25$ and estimated $f_{a,t}$ ranging from 0.009 to 1.983. We passed this fishing mortality $f_{a,t}$ and the natural mortality m to the DRM as spatially homogeneous known quantities (i.e., without error), except in the temperature-dependent model. The latter model instead estimated m in every patch and year as a combination of estimated temperature-driven mortality and a non-

temperature-related natural mortality parameter bounded at (0,0.25). The assessment estimates of f began in 1982, so we imputed the 1982 values for our earliest years of summer flounder data (1972 - 1981).

1.5 Species distribution model

To compare DRM performance to SDMs widely used in the range shift literature, we fitted a generalized additive model (GAM) SDM (Morley et al., 2018) with the "mgcv" package in R (Wood, 2017). The GAM SDM was also a two-stage model; we fitted one GAM to presences and absences in the training data using a logistic regression (i.e., logit-link and Bernoulli family) and a second GAM to log-abundance conditioned on presence, assuming a Gaussian error distribution. Both were single intercept models with a spline on bottom temperature (the sole predictor). Unlike the DRMs, we fitted the GAM to the haul-level data (not aggregated to the patch scale). As noted below (see Section 1.4), bottom temperature records were missing from a number of hauls in 2008. The interpolation method we used to fill these data gaps for the DRMs was not appropriate for the much higher spatial resolution of the GAMs, so we omitted 2008 data from the GAMs. GAMs were fitted and predicted at the scale of observations; predictions were then averaged within patches for model evaluation and comparison.

1.6 Model evaluation and comparison

We used a retrospective forecasting approach to assess model performance. The DRM was fitted to summer flounder data from 1972-2006 and then simulated for the final decade of data (2007-2016). The forecast was initialized with the final year of fishing mortality data passed to the model (2006) and then run forward by making draws from the posterior probability distribution of parameters estimated in the model fitting routine. Observed temperature data for 2007-2016 were used. We calculated summary statistics from the 2007-2016 data for forecast validation by averaging the observations into patches, as we did for the input to the DRM (Section 1.4).

To forecast into the testing decade for the GAM SDM, we passed the bottom temperature records from the testing dataset to the two parts of the GAM and multiplied their predictions together. We then aggregated the predictions to the patch scale the same way we aggregated the raw data passed to the DRM (Section 1.4) to enable forecast comparisons.

To assess DRM performance, we compared forecast metrics of geographic distribution to observations of these metrics, to the SDM forecasts, and to a persistence forecast. The persistence forecast was a continuation of the observations from the final year of the training interval (2006) into every subsequent year. The forecast metrics included (1) the abundance-weighted latitudinal range center (i.e., range centroid) and (2) the cold and (3) the warm range edge positions. The edge positions were calculated as abundance-weighted 0.05 and

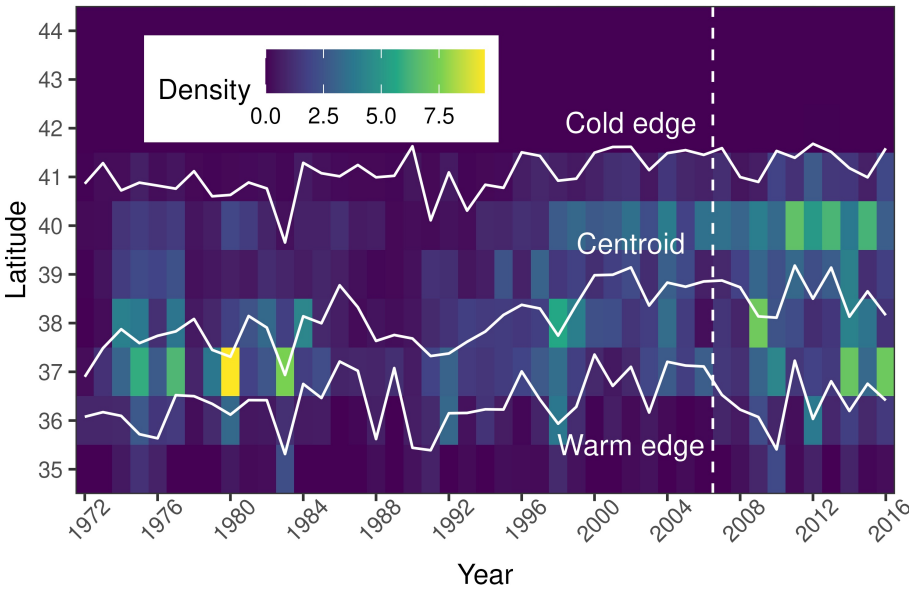

Figure 3: Summer flounder dynamics over space and time in the study region from 1972-2016. Cells are color-coded by mean density in the survey, and summary statistics used to evaluate and validate models (the position of the range centroid and warm and cold edges) are plotted.

0.95 quantiles of latitude. Note that because our study domain did not encompass the full geographic distribution of the focal species, these represented population range metrics, not metrics for the full species range.

For each of these metrics, we calculated the residuals (forecasts minus observations) in each year. We then calculated bias (mean of residuals) and root mean square error (RMSE, square root of the mean of the squared residuals) for each metric. For the DRMs, we calculated the residuals for each of 12,000 posterior draws and then used the mean residual value for each posterior to calculate bias and RMSE.

2 Results

Over the time-series, summer flounder exhibited complex spatiotemporal dynamics, including a decline in density in the 1980s and an increase beginning in the 1990s (Fig. 3). The geographic distribution was relatively stable from 1972-1990, then shifted north substantially through 2002 before another period of relative stability through 2016 (Fig. 3). During the northward shift (1990-2002), for example, the centroid shifted from the latitude of Virginia (37.7 °N) to that of New Jersey (39.1 °N), approximately 155 km (Fig. 2). These observed

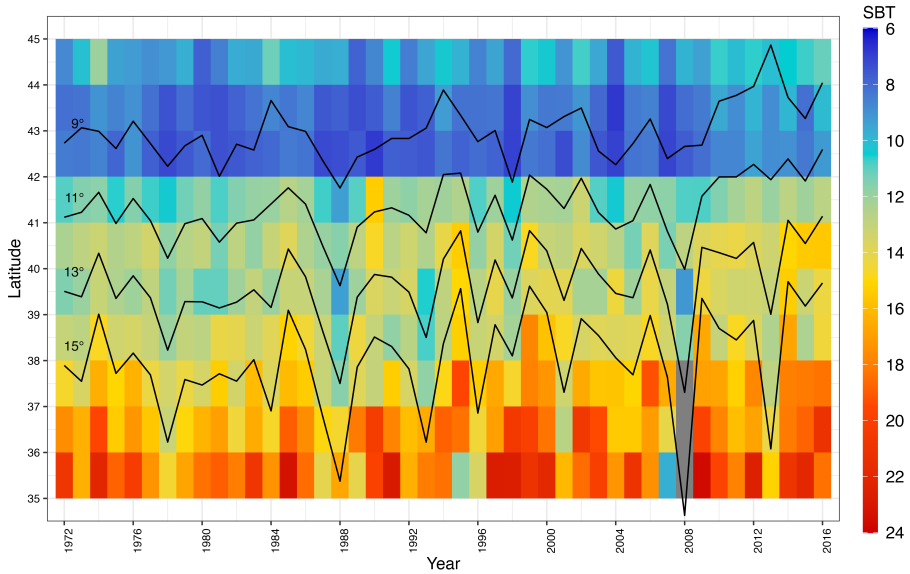

Figure 4: Sea bottom temperatures (SBT) recorded *in situ* by trawl surveys by patch and year, calculated as means of haul-level observations. Grey boxes indicate data gaps. Solid black lines represent isotherms; their positions were calculated by fitting a linear regression of latitude on temperature in each year, and predicting the annual latitudinal position of each degree Celcius value.

shifts occurred primarily during our model training interval. From 2007-2016 (our testing interval), summer flounder did not shift north significantly (linear regression of latitude on time; centroid coefficient -0.03 ± 0.05 and $p = 0.58$, warm edge coefficient 0.04 ± 0.06 and $p = 0.52$, cold edge coefficient 0.01 ± 0.03 and $p = 0.79$; $n = 10$; Fig. 3).

The *in situ* sea bottom temperature exhibited significant warming of 0.04 $\pm$ 0.003 °C per year across the study region from 1972-2016 (linear regression; p <0.001). This trend was spatially and temporally heterogeneous; warming was concentrated in the center of the study domain (Fig. 2) during the training period (Supp. Tab. 3), with a particularly strong period of warming from 1988-2000 (Fig. 4) that aligned with the strong northward shift observed in flounder (Fig. 3). During the testing decade, warming was stronger towards the northern and southern edges of the study domain, though only statistically significant at and below 40 °N (Fig. 4, Supp. Tab. 4).

Observations of summer flounder were available for 14,025 individual fish caught across 12,203 distinct hauls from 1972-2016. As is common in marine fish surveys, the data were heavily zero-inflated; 81% of these hauls did not catch any summer flounder and 96.5% of hauls caught fewer than ten summer flounder (Supp. Fig. 1). The number of hauls per year was generally between 225 and 325, although 1978 and 1979 had almost 500 (Supp. Fig. 2).

All four DRM configurations (no temperature effect, or temperature effect on recruitment, mortality, or movement) converged when fit to the data and produced density estimates consistent with observations (Supp. Fig. 3-6). The models generally reproduced the decline in density until 1990 and the increase afterwards, though the null model (no temperature effect) failed to re-create the lower abundances towards the northern and southern range edges and higher abundance in mid-latitudes (Supp. Fig. 3). The models with temperature-dependent demography, and particularly recruitment or mortality, more effectively captured these spatial gradients (Supp. Fig. 4-6). In addition, their parameter estimates differed substantially (Supp. Fig. 7). Temperature-dependent recruitment had an optimum of 14.4 – 14.6 °C with a width of 1.33 – 1.45 °C (90% credible intervals; see Eqn. 6), suggesting a narrow range of optimal temperatures for recruitment of new offspring. Temperature-dependent mortality had a similar optimum (14.6 – 14.8 °C) but a greater width (3.61 – 4.72 °C) that implied substantially less sensitivity of mortality to differences in temperature. By contrast, movement had a higher optimal temperature (16.8 – 20.1 °C) and a narrow width (1.09 – 1.33 °C), suggesting adults moved towards warmer waters than were optimal for recruitment of offspring. The temperature-dependent movement and mortality models had fairly similar estimates of the between-patch diffusion rate for adults (0.11 – 0.26 and 0.10 – 0.21, respectively), while the temperature-dependent recruitment model estimated a much lower adult diffusion rate (0.0003 – 0.02) and the null model estimated an intermediate rate (0.07 – 0.19).

The temperature-dependent recruitment forecast, the temperature-dependent mortality forecast, and the persistence forecast most often had greater skill (lower RMSE) and less bias out-of-sample than the other models tested (Fig. 5, Supp. Fig. 8). Both of these DRMs notably out-performed the persistence forecast at the warm range edge, where the persistence forecast substantially over-predicted the edge latitude. The GAM and other two DRM configurations (a temperature effect on movement, or no temperature effect) performed worse across the considered metrics, with less skill and greater bias. For the temperature-dependent recruitment DRM, with the exception of the cold edge in 2012 and the warm edge in 2010, every observed range metric fell within the 95% credible interval in every year (Fig. 6). By contrast, the GAM over-predicted the range size of summer flounder, estimating the warm edge further south and the cold edge much further north than they were found in the survey (Fig. 6). The actual spatiotemporal distribution of summer flounder in the survey from 2007-2016 was highly concentrated between 37-40°N, which was better captured by the persistence and DRM forecasts (Fig. 3).

3 Discussion

Integrating greater biological process and mechanism into forecasts of species responses to climate change and variation has long been a goal (Pagel & Schurr, 2012; Urban et al., 2016). Here, we show that dynamic range models with

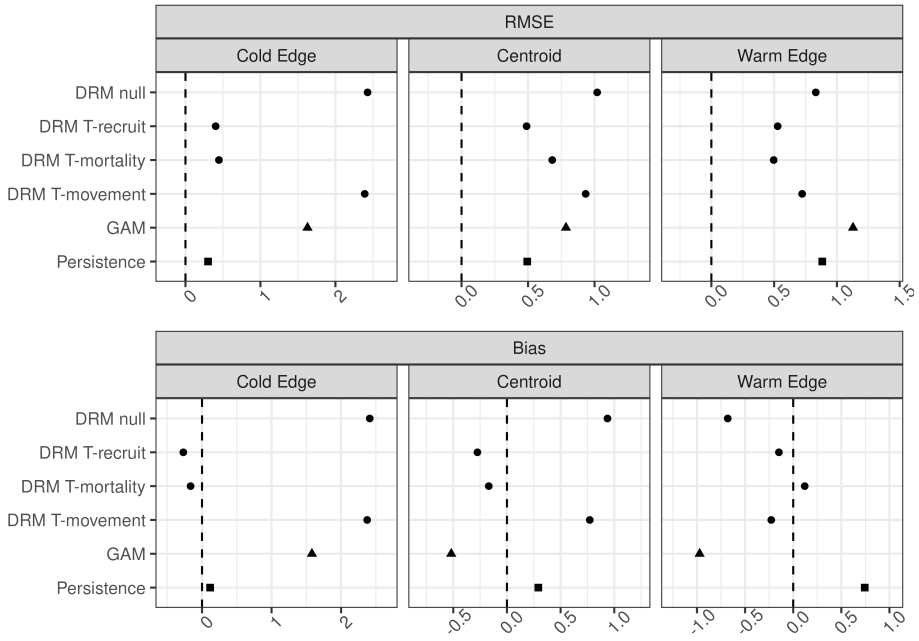

Figure 5: Skill of DRMs, GAM, and a persistence forecast at predicting summer flounder range dynamics out-of-sample from 2007-2016 measured as root mean square error (RMSE) and bias. The DRMs included no temperature effect (null) or a temperature effect on recruitment (T-recruit), mortality (T-mortality), or movement (T-movement). We measured ranged dynamics with three metrics: the warm and cold range edge positions and the centroid (abundance-weighted latitudinal average) every year. RMSE measures how close the predictions were to the observed values; lower RMSE values indicate greater accuracy. Bias measures whether the predictions were consistently too far north (positive bias) or too far south (negative bias); values closer to zero (indicated by the vertical dashed line) indicate less bias. Note that x-axis scales vary by panel.

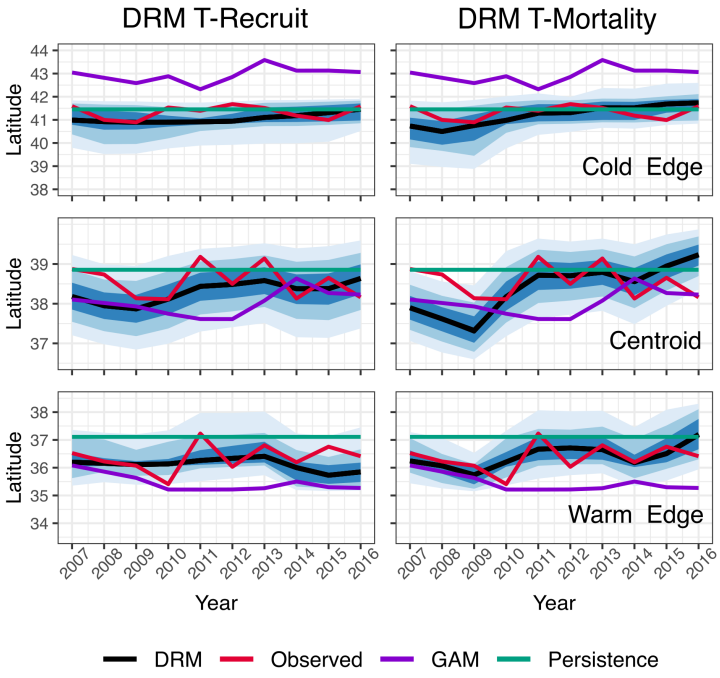

Figure 6: Observed range dynamics of summer flounder (red line) in the study domain (Fig. 2) during the testing decade (2007-2016) and range dynamics forecasted by the temperature-dependent recruitment (left) and temperature-dependent mortality (right) DRMs and by the GAM and persistence forecasts. Latitudinal positions of the cold edge (top row), range centroid (middle row), and warm edge of the population (bottom row) are shown. Shaded blue regions represent credible intervals (0.5, 0.8, and 0.95) of the DRM forecast.

climate-dependent demographic rates outperformed statistical SDMs in near-term forecasting of range dynamics during a 10-year interval of environmental variability. These results provide evidence that rates of population growth, dispersal, and reproduction are important for understanding species responses to a changing climate, especially in the common scenario where species are not in equilibrium with the climate (Guisan & Thuiller, 2005). Our approach also provided evidence that range shifts in summer flounder can be explained by temperature-dependent recruitment or mortality. Because of their Bayesian structure, the DRMs also allowed the quantification and communication of uncertainty around forecasted state variables like geographic position.

We formulated DRMs to represent alternative hypotheses for the mechanisms driving summer flounder geographic distributions. Temperature-dependent recruitment, for example, can drive northward shifts as habitats warm further north and become thermally suitable for larvae and small juveniles. A more rapid northward shift in small juvenile summer flounder than in adults has also been reported (Perretti & Thorson, 2019), consistent with a recruitment-driven shift. Alternatively, increasing rates of survival at and beyond northern range edges can also drive a northern shift in the density of the species, as suggested by the temperature-dependent mortality model. Previous research has suggested that summer flounder mortality is linked to oceanographic conditions, though that study did not try to explain the northward geographic shift in summer flounder distributions (O'Leary et al., 2019). In addition, we found evidence that adult fish prefer and move towards higher temperatures than are optimal for larvae and juveniles. This ontogenetic difference is consistent with patterns across fishes suggesting that adult high temperature limits are higher than for larvae (Dahlke et al., 2020), though inconsistent with generally lower temperature preferences in larger than in smaller fishes (Lafrance et al., 2005). More broadly, our application of DRMs provides a model for moving research on geographic range shifts more fully towards demographic and ecological mechanisms. The explicit demography in the DRMs allows them to be easily extended to include other mechanisms, including species interactions (Urban et al., 2016).

The persistence forecast—i.e., the prediction that future conditions will be identical to the final year of available data—performed relatively well in our analysis, except at the warm range edge. This result arose because the geographic range of summer flounder was remarkably stable during the testing decade despite marked environmental variability, and was unexpected given widespread observations of temperature-related range shifts in marine fishes in this region (Fredston et al., 2021; Fredston-Hermann et al., 2020; Mills et al., 2024; Pinsky et al., 2013). However, temporal autocorrelation in biological systems (often termed "ecological memory") is common and often used to inform statistical models of near-term change (Ogle et al., 2015; Wolkovich et al., 2014). Indeed, the time horizon of 1-10 years that we selected for its management relevance may be uniquely difficult to predict, being longer than the daily-to-annual lead times of most near-term forecasting programs (Dietze et al., 2018) but shorter than mid- and end-century projections that ignore transient population dynamics (Morley et al., 2018). Other studies at this time hori-

zon have found that persistence forecasts performed similarly to, or even better than, mechanistic models (Harris et al., 2018; Ward et al., 2014).

The DRM estimated a large number of parameters, including some that are difficult to estimate, such the diffusion rate between habitat patches. We emphasize that the primary purpose of this model is predictive, not providing precise estimates of population parameters as would be done in a spatial stock assessment model (Punt, 2019) which share many of the same processes and data fitting concepts. This distinction matters because the performance of a primarily predictive model can be judged relative to alternatives, as we did here. In contrast, a model based primarily around inference needs to be able to demonstrate that it can reliably identify the individual estimated parameters, which we have not rigorously explored (Tredennick et al., 2021).

Dynamic range models that represent biological processes can and should be extended to a wide range of taxa and systems that are underrepresented in the literature on forecasting biodiversity responses to global change (Urban et al., 2022; Zurell et al., 2022).One advantage of the DRM approach is that, like other mechanistic models, it can in theory capture any ecological process for which one can write down an equation hypothesizing its effect on a population parameter (Pagel & Schurr, 2012). Another advantage is that DRMs are conducive to best practices in informing environmental decision-making, including mechanistic representation of causal linkages, selection of model structure for management relevance, measurement of forecast skill with decision-relevant metrics, and quantification of uncertainty (Bodner et al., 2021; Mason et al., 2023; Schmolke et al., 2010; Schuwirth et al., 2019). We focused on testing mechanisms of temperature dependence and fishing for a single species as a case study; future work can incorporate new processes such as local adaptation or test the DRM against more species with different life histories. Methodological investigations of dynamic range modeling are also needed, including the effect of spatial and temporal scale and extent on projections, and incorporating multiple observational data streams. For the summer flounder DRM to be operational as a future (rather than retrospective) forecasting system, additional work would be needed to incorporate future temperature projections (e.g., Koul et al., 2024). Given the limited use to date of mechanistic models that are both validated against historical observations and ready to forecast species on the move, we hope that the results here motivate further investment in this promising new field.

4 Acknowledgments

The Mid-Atlantic Fishery Management Council and its Scientific and Statistical Committee and Ecosystem and Ocean Planning Committee and Advisory Panel all provided feedback on the management applications of this work. Funding was provided by Lenfest Ocean Program grant 00032755 (ALF and MLP); NSERC Discovery Grant (Grant No. RGPIN-2022-04559), NSERC Discovery Launch Supplement (Grant No: DGECR-2022-00454) and NSERC Postdoctoral Fel-

lowship (JK); and US National Science Foundation grants #OCE-1426891 and #CBET-2137701 (MLP). We also thank Emily Moberg for early discussions on model development and Benjamin Parzych for summer flounder drawings.

References

Bodner, K., Rauen Firkowski, C., Bennett, J. R., Brookson, C., Dietze, M., Green, S., Hughes, J., Kerr, J., Kunegel-Lion, M., Leroux, S. J., McIntire, E., Molnár, P. K., Simpkins, C., Tekwa, E., Watts, A., & Fortin, M.-J. (2021). Bridging the divide between ecological forecasts and environmental decision making [_eprint: https://onlinelibrary.wiley.com/doi/pdf/10.1002/ecs2.3869]. *Ecosphere*, *12*(12), e03869. https://doi.org/10.1002/ecs2.3869

Briscoe, N. J., Elith, J., Salguero-Gómez, R., Lahoz-Monfort, J. J., Camac, J. S., Giljohann, K. M., Holden, M. H., Hradsky, B. A., Kearney, M. R., McMahon, S. M., Phillips, B. L., Regan, T. J., Rhodes, J. R., Vesk, P. A., Wintle, B. A., Yen, J. D. L., & Guillera-Arroita, G. (2019). Forecasting species range dynamics with process-explicit models: Matching methods to applications. *Ecology Letters*, *22*(11), 1940–1956. https://doi.org/10.1111/ele.13348

Brodie, S., Smith, J. A., Muhling, B. A., Barnett, L. A. K., Carroll, G., Fiedler, P., Bograd, S. J., Hazen, E. L., Jacox, M. G., Andrews, K. S., Barnes, C. L., Crozier, L. G., Fiechter, J., Fredston, A., Haltuch, M. A., Harvey, C. J., Holmes, E., Karp, M. A., Liu, O. R., … Kaplan, I. C. (2022). Recommendations for quantifying and reducing uncertainty in climate projections of species distributions [_eprint: https://onlinelibrary.wiley.com/doi/pdf/10.1111/gcb.16371]. *Global Change Biology*, *28*(22), 6586–6601. https://doi.org/10.1111/gcb.16371

Cabral, J. S., Valente, L., & Hartig, F. (2017). Mechanistic simulation models in macroecology and biogeography: State-of-art and prospects [_eprint: https://onlinelibrary.wiley.com/doi/pdf/10.1111/ecog.02480]. *Ecography*, *40*(2), 267–280. https://doi.org/10.1111/ecog.02480

Dahlke, F. T., Wohlrab, S., Butzin, M., & Pörtner, H.-O. (2020). Thermal bottlenecks in the life cycle define climate vulnerability of fish [Publisher: American Association for the Advancement of Science Section: Research Article]. *Science*, *369*(6499), 65–70. https://doi.org/10.1126/science.aaz3658

Davis, A. J., Jenkinson, L. S., Lawton, J. H., Shorrocks, B., & Wood, S. (1998). Making mistakes when predicting shifts in species range in response to global warming. *Nature*, *391*(6669), 783–786. https://doi.org/10.1038/35842

Dietze, M. C., Fox, A., Beck-Johnson, L. M., Betancourt, J. L., Hooten, M. B., Jarnevich, C. S., Keitt, T. H., Kenney, M. A., Laney, C. M., Larsen, L. G., Loescher, H. W., Lunch, C. K., Pijanowski, B. C., Randerson, J. T., Read, E. K., Tredennick, A. T., Vargas, R., Weathers, K. C., & White, E. P. (2018). Iterative near-term ecological forecasting: Needs,

opportunities, and challenges. *Proceedings of the National Academy of Sciences*, *115*(7), 1424–1432. https://doi.org/10.1073/pnas.1710231115

Ehrlén, J., & Morris, W. F. (2015). Predicting changes in the distribution and abundance of species under environmental change. *Ecology Letters*, *18*(3), 303–314. https://doi.org/10.1111/ele.12410

Elith, J., & Leathwick, J. R. (2009). Species Distribution Models: Ecological Explanation and Prediction Across Space and Time. *Annual Review of Ecology, Evolution, and Systematics*, *40*(1), 677–697. https://doi.org/10.1146/annurev.ecolsys.110308.120159

Evans, M. E. K., Merow, C., Record, S., McMahon, S. M., & Enquist, B. J. (2016). Towards Process-based Range Modeling of Many Species. *Trends in Ecology & Evolution*, *31*(11), 860–871. https://doi.org/10.1016/j.tree.2016.08.005

Forrest, D., Stuart, M., & Pinsky, M. L. (2020). Scripts and data f or OceanAdapt website to visualize shifts in marine animal distributions: Update 2020. https://doi.org/10.5281/zenodo.3885625

Fredston, A., Pinsky, M., Selden, R. L., Szuwalski, C., Thorson, J. T., Gaines, S. D., & Halpern, B. S. (2021). Range edges of North American marine species are tracking temperature over decades [_eprint: https://onlinelibrary.wiley.com/doi/pdf/10.1111 *Global Change Biology*, *27*(13), 3145–3156. https://doi.org/10.1111/gcb.15614

Fredston-Hermann, A., Selden, R., Pinsky, M., Gaines, S. D., & Halpern, B. S. (2020). Cold range edges of marine fishes track climate change better than warm edges [_eprint: https://onlinelibrary.wiley.com/doi/pdf/10.1111/gcb.15035]. *Global Change Biology*, *26*(5), 2908–2922. https://doi.org/10.1111/gcb.15035

Gabry, J., Češnovar, R., Johnson, A., & Bronder, S. (2024). *Cmdstanr: R Interface to 'CmdStan'*.

Guisan, A., & Thuiller, W. (2005). Predicting species distribution: Offering more than simple habitat models [WOS:000231224600011]. *Ecology Letters*, *8*(9), 993–1009. https://doi.org/10.1111/j.1461-0248.2005.00792.x

Harris, D. J., Taylor, S. D., & White, E. P. (2018). Forecasting biodiversity in breeding birds using best practices. *PeerJ*, *6*. https://doi.org/10.7717/peerj.4278

Jarnevich, C. S., Stohlgren, T. J., Kumar, S., Morisette, J. T., & Holcombe, T. R. (2015). Caveats for correlative species distribution modeling. *Ecological Informatics*, *29*, 6–15. https://doi.org/10.1016/j.ecoinf.2015.06.007

Johnson, K. F., Councill, E., Thorson, J. T., Brooks, E., Methot, R. D., & Punt, A. E. (2016). Can autocorrelated recruitment be estimated using integrated assessment models and how does it affect population forecasts? *Fisheries Research*, *183*, 222–232. https://doi.org/10.1016/j.fishres.2016.06.004

Kearney, M., & Porter, W. (2009). Mechanistic niche modelling: Combining physiological and spatial data to predict species' ranges. *Ecology Letters*, *12*(4), 334–350. https://doi.org/10.1111/j.1461-0248.2008.01277.x

Koul, V., Ross, A. C., Stock, C., Zhang, L., Delworth, T., & Wittenberg, A. (2024). A Predicted Pause in the Rapid Warming of the Northwest Atlantic Shelf in the Coming Decade [_eprint: https://onlinelibrary.wiley.com/doi/pdf/10.1029/2024GL11 *Geophysical Research Letters*, *51*(17), e2024GL110946. https://doi.org/10.1029/2024GL110946

Lafrance, P., Castonguay, M., Chabot, D., & Audet, C. (2005). Ontogenetic changes in temperature preference of Atlantic cod [_eprint: https://onlinelibrary.wiley.com/doi/pdf/10.1 1112.2005.00623.x]. *Journal of Fish Biology*, *66*(2), 553–567. https://doi.org/10.1111/j.0022-1112.2005.00623.x

Laubmeier, A. N., Cazelles, B., Cuddington, K., Erickson, K. D., Fortin, M.-J., Ogle, K., Wikle, C. K., Zhu, K., & Zipkin, E. F. (2020). Ecological Dynamics: Integrating Empirical, Statistical, and Analytical Methods. *Trends in Ecology & Evolution*. https://doi.org/10.1016/j.tree.2020.08.006

Le Squin, A., Boulangeat, I., & Gravel, D. (2021). Climate-induced variation in the demography of 14 tree species is not sufficient to explain their distribution in eastern North America [_eprint: https://onlinelibrary.wiley.com/doi/pdf/10.1111/geb.13209]. *Global Ecology and Biogeography*, *30*(2), 352–369. https://doi.org/10.1111/geb.13209

Lee-Yaw, J. A., L. McCune, J., Pironon, S., & N. Sheth, S. (2022). Species distribution models rarely predict the biology of real populations [_eprint: https://onlinelibrary.wiley.com/doi/pdf/10.1111/ecog.05877]. *Ecography*, *2022*(6), e05877. https://doi.org/10.1111/ecog.05877

Mason, J. G., Weisberg, S. J., Morano, J. L., Bell, R. J., Fitchett, M., Griffis, R. B., Hazen, E. L., Heyman, W. D., Holsman, K., Kleisner, K. M., Westfall, K., Conrad, M. K., Daly, M., Golden, A. S., Harvey, C. J., Kerr, L. A., Kirchner, G., Levine, A., Lewison, R. L., … Stram, D. L. (2023). Linking knowledge and action for climate-ready fisheries: Emerging best practices across the US. *Marine Policy*, *155*, 105758. https://doi.org/10.1016/j.marpol.2023.105758

Maureaud, A., Abrantes, J. P., Kitchel, Z., Mannocci, L., Pinsky, M., Fredston, A., Beukhof, E., Forrest, D., Frelat, R., Palomares, D., Pecuchet, L., Thorson, J., Denderen, D. v., & Merigot, B. (2023). FishGlob_data: An integrated database of fish biodiversity sampled with scientific bottom-trawl surveys. https://doi.org/10.31219/osf.io/2bcjw

Mills, K. E., Kemberling, A., Kerr, L. A., Lucey, S. M., McBride, R. S., Nye, J. A., Pershing, A. J., Barajas, M., & Lovas, C. S. (2024). Multispecies population-scale emergence of climate change signals in an ocean warming hotspot. *ICES Journal of Marine Science*, fsad208. https://doi.org/10.1093/icesjms/fsad208

Morley, J. W., Selden, R. L., Latour, R. J., Frölicher, T. L., Seagraves, R. J., & Pinsky, M. L. (2018). Projecting shifts in thermal habitat for 686 species on the North American continental shelf [Publisher: Public Library of Science]. *PLOS ONE*, *13*(5), e0196127. https://doi.org/10.1371/journal.pone.0196127

Mouquet, N., Lagadeuc, Y., Devictor, V., Doyen, L., Duputié, A., Eveillard, D., Faure, D., Garnier, E., Gimenez, O., Huneman, P., Jabot, F., Jarne, P., Joly, D., Julliard, R., Kéfi, S., Kergoat, G. J., Lavorel, S., Le Gall, L., Meslin, L., … Loreau, M. (2015). Predictive ecology in a changing world. *Journal of Applied Ecology*, *52*(5), 1293–1310. https://doi.org/10.1111/1365-2664.12482

NEFSC. (2019). *66th Northeast Regional Stock Assessment Workshop (66th SAW) Assessment Report* (tech. rep. Northeast Fish Sci Cent Ref Doc. 19-08). Northeast Fisheries Science Center.

Ogle, K., Barber, J. J., Barron-Gafford, G. A., Bentley, L. P., Young, J. M., Huxman, T. E., Loik, M. E., & Tissue, D. T. (2015). Quantifying ecological memory in plant and ecosystem processes [_eprint: https://onlinelibrary.wiley.com/doi/pdf/10.1111/ele *Ecology Letters*, *18*(3), 221–235. https://doi.org/10.1111/ele.12399

O'Leary, C. A., Miller, T. J., Thorson, J. T., & Nye, J. A. (2019). Understanding historical summer flounder (Paralichthys dentatus) abundance patterns through the incorporation of oceanography-dependent vital rates in Bayesian hierarchical models [Publisher: NRC Research Press]. *Canadian Journal of Fisheries and Aquatic Sciences*, *76*(8), 1275–1294. https://doi.org/10.1139/cjfas-2018-0092

Osada, Y., Kuriyama, T., Asada, M., Yokomizo, H., & Miyashita, T. (2019). Estimating range expansion of wildlife in heterogeneous landscapes: A spatially explicit state-space matrix model coupled with an improved numerical integration technique [_eprint: https://onlinelibrary.wiley.com/doi/pdf/10.1002/ece3.4739]. *Ecology and Evolution*, *9*(1), 318–327. https://doi.org/10.1002/ece3.4739

Pagel, J., & Schurr, F. M. (2012). Forecasting species ranges by statistical estimation of ecological niches and spatial population dynamics. *Global Ecology and Biogeography*, *21*(2), 293–304. https://doi.org/10.1111/j.1466-8238.2011.00663.x

Parmesan, C., & Yohe, G. (2003). A globally coherent fingerprint of climate change impacts across natural systems. *Nature*, *421*(6918), 37–42. https://doi.org/10.1038/nature01286

Pearson, R. G., & Dawson, T. P. (2003). Predicting the impacts of climate change on the distribution of species: Are bioclimate envelope models useful? [_eprint: https://onlinelibrary.wiley.com/doi/pdf/10.1046/j.1466-822X.2003.00042.x]. *Global Ecology and Biogeography*, *12*(5), 361–371. https://doi.org/10.1046/j.1466-822X.2003.00042.x

Pecl, G. T., Araújo, M. B., Bell, J. D., Blanchard, J., Bonebrake, T. C., Chen, I.-C., Clark, T. D., Colwell, R. K., Danielsen, F., Evengård, B., Falconi, L., Ferrier, S., Frusher, S., Garcia, R. A., Griffis, R. B., Hobday, A. J., Janion-Scheepers, C., Jarzyna, M. A., Jennings, S., … Williams, S. E. (2017). Biodiversity redistribution under climate change: Impacts on ecosystems and human well-being. *Science*, *355*(6332), eaai9214. https://doi.org/10.1126/science.aai9214

Perretti, C. T., & Thorson, J. T. (2019). Spatio-temporal dynamics of summer flounder (Paralichthys dentatus) on the Northeast US shelf. *Fisheries Research*, *215*, 62–68. https://doi.org/10.1016/j.fishres.2019.03.006

Pinsky, M. L., Selden, R. L., & Kitchel, Z. J. (2020). Climate-Driven Shifts in Marine Species Ranges: Scaling from Organisms to Communities. *Annual Review of Marine Science*, *12*(1). https://doi.org/10.1146/annurev-marine-010419-010916

Pinsky, M. L., Worm, B., Fogarty, M. J., Sarmiento, J. L., & Levin, S. A. (2013). Marine taxa track local climate velocities. *Science*, *341*(6151), 1239–1242.

Punt, A. E. (2019). Spatial stock assessment methods: A viewpoint on current issues and assumptions. *Fisheries Research*, *213*, 132–143. https://doi.org/10.1016/j.fishres.2019.01.014

Rubenstein, M. A., Weiskopf, S. R., Bertrand, R., Carter, S. L., Comte, L., Eaton, M. J., Johnson, C. G., Lenoir, J., Lynch, A. J., Miller, B. W., Morelli, T. L., Rodriguez, M. A., Terando, A., & Thompson, L. M. (2023). Climate change and the global redistribution of biodiversity: Substantial variation in empirical support for expected range shifts. *Environmental Evidence*, *12*(1), 7. https://doi.org/10.1186/s13750-023-00296-0

Schmolke, A., Thorbek, P., DeAngelis, D. L., & Grimm, V. (2010). Ecological models supporting environmental decision making: A strategy for the future. *Trends in Ecology & Evolution*, *25*(8), 479–486. https://doi.org/10.1016/j.tree.2010.05.001

Schuwirth, N., Borgwardt, F., Domisch, S., Friedrichs, M., Kattwinkel, M., Kneis, D., Kuemmerlen, M., Langhans, S. D., Martínez-López, J., & Vermeiren, P. (2019). How to make ecological models useful for environmental management. *Ecological Modelling*, *411*, 108784. https://doi.org/10.1016/j.ecolmodel.2019.108784

Smith, T. D. (2002). The Woods Hole bottom-trawl resource survey: Development of fisheries-independent multispecies monitoring [Publisher: ICES]. https://doi.org/10.17895/ICES.PUB.8888

Sunday, J. M., Bates, A. E., & Dulvy, N. K. (2012). Thermal tolerance and the global redistribution of animals. *Nature Climate Change*, *2*(9), 686–690. https://doi.org/10.1038/nclimate1539

Team, S. D. (2022). Stan Modeling Language Users Guide and Reference Manual.

Thorson, J. T., Barbeaux, S. J., Goethel, D. R., Kearney, K. A., Laman, E. A., Nielsen, J. K., Siskey, M. R., Siwicke, K., & Thompson, G. G. (2021). Estimating fine-scale movement rates and habitat preferences using multiple data sources [_eprint: https://onlinelibrary.wiley.com/doi/pdf/10.1111/faf.12592]. *Fish and Fisheries*, *22*(6), 1359–1376. https://doi.org/10.1111/faf.12592

Tredennick, A. T., Hooker, G., Ellner, S. P., & Adler, P. B. (2021). A practical guide to selecting models for exploration, inference, and prediction in

ecology [_eprint: https://esajournals.onlinelibrary.wiley.com/doi/pdf/10.1002/ecy.3336]. *Ecology*, *102*(6), e03336. https://doi.org/10.1002/ecy.3336

Urban, M. C., Bocedi, G., Hendry, A. P., Mihoub, J.-B., Pe'er, G., Singer, A., Bridle, J. R., Crozier, L. G., Meester, L. D., Godsoe, W., Gonzalez, A., Hellmann, J. J., Holt, R. D., Huth, A., Johst, K., Krug, C. B., Leadley, P. W., Palmer, S. C. F., Pantel, J. H., … Travis, J. M. J. (2016). Improving the forecast for biodiversity under climate change. *Science*, *353*(6304), aad8466. https://doi.org/10.1126/science.aad8466

Urban, M. C., Travis, J. M. J., Zurell, D., Thompson, P. L., Synes, N. W., Scarpa, A., Peres-Neto, P. R., Malchow, A.-K., James, P. M. A., Gravel, D., De Meester, L., Brown, C., Bocedi, G., Albert, C. H., Gonzalez, A., & Hendry, A. P. (2022). Coding for Life: Designing a Platform for Projecting and Protecting Global Biodiversity. *BioScience*, *72*(1), 91–104. https://doi.org/10.1093/biosci/biab099

Ward, E. J., Holmes, E. E., Thorson, J. T., & Collen, B. (2014). Complexity is costly: A meta-analysis of parametric and non-parametric methods for short-term population forecasting [_eprint: https://onlinelibrary.wiley.com/doi/pdf/10.1111/j.1600-0706.2014.00916.x]. *Oikos*, *123*(6), 652–661. https://doi.org/10.1111/j.1600-0706.2014.00916.x

Wolkovich, E. M., Cook, B. I., McLauchlan, K. K., & Davies, T. J. (2014). Temporal ecology in the Anthropocene [_eprint: https://onlinelibrary.wiley.com/doi/pdf/10.1111/ele.12353] *Ecology Letters*, *17*(11), 1365–1379. https://doi.org/10.1111/ele.12353

Wood, S. N. (2017). *Generalized Additive Models: An Introduction with R* (2nd ed.). Chapman; Hall/CRC.

Zurell, D. (2017). Integrating demography, dispersal and interspecific interactions into bird distribution models [_eprint: https://onlinelibrary.wiley.com/doi/pdf/10.1111/jav.01225] *Journal of Avian Biology*, *48*(12), 1505–1516. https://doi.org/https://doi.org/10.1111/jav.01225

Zurell, D., König, C., Malchow, A.-K., Kapitza, S., Bocedi, G., Travis, J., & Fandos, G. (2022). Spatially explicit models for decision-making in animal conservation and restoration [_eprint: https://onlinelibrary.wiley.com/doi/pdf/10.1111/ecog.05787]. *Ecography*, *2022*(4). https://doi.org/10.1111/ecog.05787

Zurell, D., Thuiller, W., Pagel, J., Cabral, J. S., Münkemüller, T., Gravel, D., Dullinger, S., Normand, S., Schiffers, K. H., Moore, K. A., & Zimmermann, N. E. (2016). Benchmarking novel approaches for modelling species range dynamics. *Global Change Biology*, *22*(8), 2651–2664. https://doi.org/10.1111/gcb.13251